





Double optical gating for generating high flux isolated attosecond pulses in the soft X-ray regime

JIE LI,^{1,2,3}  ANDREW CHEW,¹ SHUYUAN HU,¹ JONATHON WHITE,¹ XIAOMING REN,¹ SEUNGHWOI HAN,¹  YANCHUN YIN,¹  YANG WANG,¹ YI WU,¹  AND ZENGHU CHANG^{1,*}

¹*Institute for the Frontier of Attosecond Science and Technology, CREOL and Department of Physics, University of Central Florida, Orlando, Florida 32816, USA*

²*Academy of Opto-Electronics, Chinese Academy of Sciences, Beijing 100094, China*

³*School of Optoelectronics, University of the Chinese Academy of Sciences, Beijing 100049, China*

**Zenghu.Chang@ucf.edu*

Abstract: Double optical gating (DOG) technique was implemented with a two-cycle, 1.7 μm driving field to generate isolated attosecond pulses in the 100–250 eV spectrum range. The strong ellipticity dependency of the high harmonics from the 1.7 μm driving field makes polarization based gating method very efficient. When a second harmonic (SH) field is introduced, complete gating can be achieved with less ionization from the leading edge of the driving field, which yields supercontinua with a pulse energy of 0.3 nJ. We perform an attosecond streaking measurement to confirm the generation of isolated attosecond pulses.

© 2019 Optical Society of America under the terms of the [OSA Open Access Publishing Agreement](#)

1. Introduction

Attosecond pulses can be generated from an extreme nonlinear process called high harmonic generation (HHG) [1,2]. The HHG photon energy can be tailored from the XUV to soft X-rays based on its driving laser source and the interaction media [3]. Combined with its unique sub-femtosecond temporal feature, attosecond sources have become powerful tools for studying electron dynamics and correlations in atoms, molecules and condensed matter [4].

The generation of isolated attosecond pulses (IAPs) requires sub-cycle gating techniques. The amplitude gating (AP) [5] and ionization gating (IG) [6] techniques rely on the spectral selection of cutoff harmonics driven by a strong half-cycle of the laser field. The polarization gating (PG) [7] and double optical gating (DOG) [8] techniques require a driving field that is linearly polarized in the middle and elliptically polarized elsewhere. The recombination probability of an electron recolliding with the parent ion drops with increasing field ellipticity [9,10]. As a result, only one effective recollision event occurs in the middle of the driving field, creating a temporal “switch on” for attosecond burst in only half-cycle. Unlike spectral filtering method where isolated attosecond pulses are generated only in the cutoff range, polarization based temporal gating techniques could generate an ultra-broadband spectrum covering both the plateau and cutoff harmonics. This is only true for two-cycle or longer driving pulses. When the driving pulse duration is less than a single cycle, amplitude gating become very effective because one strong recollision event dominates the photon emission process [5]. For few-cycle driving pulses, temporal gating is also possible when take in to account the propagation effect. By controlling the ionization rate of neutral atoms, effective phase match [11] and attosecond burst can be limited to only half optical cycle [12]. A relatively new isolation method, known as “attosecond lighthouse” [13,14], can also produce ultra-broadband spectra with a multicycle driving field. It creates a wavefront rotation of the driving field to angularly separate each attosecond pulse in the far field.

The implementation of various gating methods with 0.8 μm femtosecond Ti:Sapphire laser sources have demonstrated many milestone achievements in the XUV spectrum range [5,15]. Although the semiclassical model predicts that the HHG cutoff photon energy can be increased by using a higher laser intensity [9], generating high photon flux also requires macroscopic phase match, which is achieved by using a moderate laser intensity. As a result, the photon energy cutoff produced in most experiments was typically below 150 eV.

A more practical way to scale up cutoff photon energy is to use long wavelength driving lasers [16]. Few-cycle, carrier-envelope phase (CEP) stable mid-infrared (IR) sources centered at 1.6–2.1 μm are widely available now with mJ-level pulse energy. Driving high harmonic generation with these laser sources makes ultrafast spectroscopy possible in the soft X-ray regime [17,18] and IAPs were also demonstrated recently [12,19–22]. However, the energy conversion efficiency barely reaches 10^{-8} , yielding a few picojoules of soft X-ray pulses with expensive mJ-level driving laser. One reason is the unfavorable scaling of the HHG yield ($\sim \lambda^{-6}$) with longer driving wavelength [23]. This can be mitigated by using a higher gas media density and by careful control of the phase match. Another reason is the inevitable efficiency lost during the gating process. Whereas AP and IG discard the strongest plateau harmonics, PG and DOG gate a portion of the electric field with the highest absolute amplitudes to generate high harmonics. This is the main reason for low yield of the IAPs when gating techniques are applied with a multicycle driving field.

Fortunately, the gating threshold ellipticity for isolating an IAP decreases with a longer-wavelength driving field [24] and hence, PG and DOG are more effective for mid-IR sources at 1.6–2.1 μm . To generate an IAP, the gate width δt_G should be shorter than the spacing between adjacent attosecond bursts. For a linearly polarized driving field, the corresponding attosecond bursts have a half-cycle periodicity ($T_0/2$). Therefore, the PG gate width should be less than half-cycle. DOG is a combination of two-color gating [25] and PG. The second harmonic (SH) field in the two-color gating breaks the symmetry of the fundamental driving field and increases the attosecond bursts periodicity from every half-cycle to a full-cycle. As a result, the DOG gate width can be increased to a full-cycle. This will reduce the ratio of elliptical polarized field and concentrate more energy in the center of gate for driving IAPs.

In this letter, we have demonstrated the experimental feasibility of using the DOG technique at 1.7 μm to generate high energy soft X-ray IAPs covering both the plateau and the cutoff spectrum range. A CEP scan was performed to show a clear 2π -phase periodicity of HHG yield, which verifies a sufficient SH field strength. An attosecond streaking measurement was performed to confirm the generation of the IAPs. The pulse energy of the IAPs reached ~ 0.3 nJ, corresponding to a flux of $\sim 1.5 \times 10^7$ photons per laser shot in the 100–250 eV range.

2. Double optical gating for 1.7 μm driving field.

The setup for DOG experiment is illustrated in Fig. 1. The driving laser is a home-built 1 kHz, CEP-stabilized Optical Parametric Chirped Pulse Amplification (OPCPA) system with a pulse duration of 12 fs, which corresponds to a two-cycle pulse at 1.7 μm [26]. The input mid-IR field is horizontally polarized. In our DOG setup, the optical axis of the first quartz plate (198 μm) is set at 45° with respect to the input field polarization. The birefringence effect ($n_o < n_e$) introduces +1 cycle of phase delay between the o- and e- field (Fig. 1(a)). The relative difference between phase delay and group delay is only 1.7%, which was neglected in this experiment.

The beam then passes through a second 405 μm thick quartz plate with its o-axis aligned vertically. It introduces +2 cycles of phase delay between the vertically and the horizontally polarized fields. The beam is then loosely focused by a CaF_2 lens with 450 mm focus length. Inside the vacuum chamber, a 192 μm thick BBO crystal is placed 100 mm before the focus. The BBO is cut at 21° for type I (ooe) phase matching to generate a SH field centered at 0.85 μm . The o-axis of the BBO crystal is aligned vertically and orthogonal to the driving field

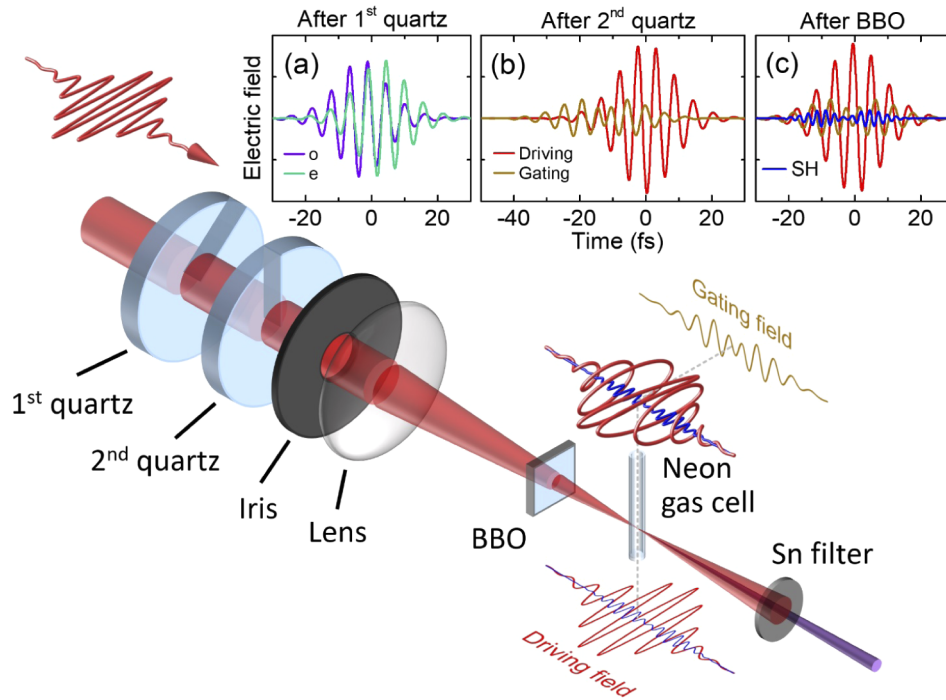


Fig. 1. Experiment setup for double optical gating. (a) The o- and e-field after the 1st quartz plate. (b) The driving and gating fields after the 2nd quartz plate. (c) The driving, gating and SH fields after the BBO crystal.

polarization. Since the BBO is a negative uniaxial crystal ($n_o > n_e$), it introduces -1.75 cycles of phase delay between the vertically and the horizontally polarized fields (Fig. 1(b)). Due to the relative thinness of the BBO crystal, the SH efficiency is less sensitive to the angle change. The BBO angle is fine-tuned to achieve a final net phase delay of +0.25 cycle. Therefore, the second quartz plate and the BBO crystal work together as a zero-order quarter wave plate.

After the BBO crystal, the o- and e-field converted into two counter-rotating circularly polarized fields with the same group delay of one cycle. These fields can also be resolved into a horizontally polarized driving field and a vertically polarized gating field (Fig. 1(c)). The SH field is produced by the gating field through type I interaction, and thus it is polarized orthogonally to the gating field and parallel to the driving field. The SH field envelope also follows the intensity of the gating field. The group delay between the SH field and the gating field is estimated to be 2 fs based on their group velocities inside the BBO crystal. This delay is important to maintain a sufficient SH strength in the middle of the PG gate. In our case, an integer multiple of half-cycle delays is introduced by the first quartz plate. As a result, the field in the middle of the PG gate is polarized in the same direction as the input field. This is important for polarization sensitive experiments since the HHG polarization follows the polarization of the driving field.

The PG or DOG gate width δt_G is determined by the time-dependent field ellipticity and can be expressed as [27]

$$\delta t_G = \frac{\varepsilon_{th} \tau_p^2}{\ln(2) T_d} \quad (1)$$

Where $T_d = T_0 = 5.3$ fs is the group delay between the o- and e-field introduced by the 1st quartz plate. $\tau_p = 12$ fs is the laser pulse duration. ε_{th} is the threshold ellipticity, define as the field ellipticity where the high harmonic yield is suppressed by 90%. For 1.7 μm driving field, the

threshold ellipticity $\varepsilon_{th} = 0.1$ [28]. Therefore, the gate width for one-cycle delay is calculated to be $\delta t_{G1} = 3.6$ fs. In DOG, the attosecond bursts have a full-cycle spacing with sufficient SH field strength. The gate width $\delta t_{G1} < T_0$ satisfies the condition of a complete gate.

3. Isolated attosecond pulses in the soft X-ray regime.

The HHG signal is generated inside a 1.5 mm-long glass capillary filled with 1 bar of neon gas. The HHG photon spectrum is collected by a soft X-ray grating spectrometer design for 50–350 eV. The photoelectron signal is recorded using a home-built attosecond streaking camera setup. The details of our detection systems have been discussed elsewhere [20].

Figure 2(a) shows the HH spectra as a function of CEP under one-cycle delay DOG. A 2π CEP periodicity is clear evidence of sufficient SH field strength in the middle of the gate. No center-of-energy motion is observed from the supercontinua while changing the CEP, which indicates our DOG is work at temporary-gating regime rather than amplitude-gating regime [29]. An attosecond streaking measurement was performed to verify the generation of IAPs (Fig. 2(b)). No backward streaking was observed, which indicates IAPs in the soft X-ray spectrum range. In the streaking experiment, helium was chosen as the detection gas to avoid photoelectron signal from different shells.

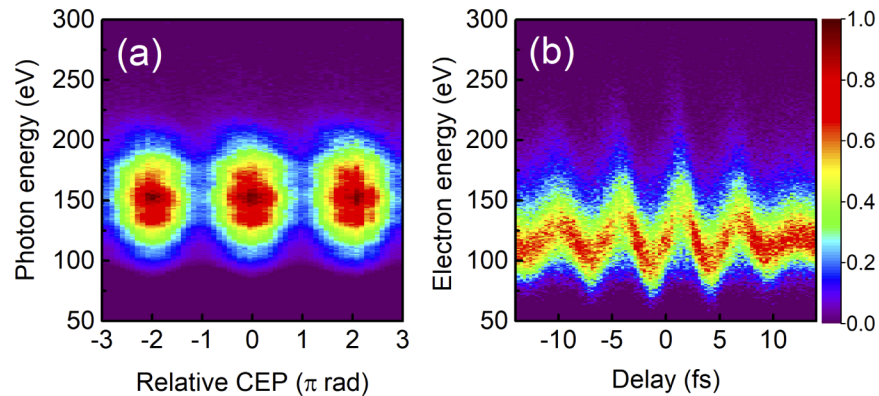


Fig. 2. (a) CEP influence on the supercontinua generation using one-cycle delay DOG. (b) Photoelectron spectrogram as a function of temporal delay between the soft X-ray and the streaking mid-IR pulses. A 100-nm-tin filter is used in the soft X-ray beam. A negative delay corresponds to an earlier mid-IR pulse arrival.

We applied the neural network retrieval method [30] to retrieve the spectral phase of the IAPs. Multiple set of simulated streaking trace are used as training data to train the neural networks. one of the trained networks is used first to perform the spectrum phase retrieval and to reconstruct a streaking trace from the measured one in Fig. 2(b). After that, 30 individually trained neural networks are applied to this reconstructed trace. The 30 different retrieval results are then used to calculate the spectrum phase error and the standard deviation of pulse duration (Fig. 3). With a similar spectrum shape and cutoff photon energy, the reconstructed 305 as pulse duration is consistent with the one generated by the PG method [20]. Since the intrinsic chirp from the HHG is inversely proportional to the driving laser wavelength [31], using long wavelength mid-IR laser can reduce the attochirp for a certain photon energy.

To compare the photon flux with our previous work [20], we use a diffraction grating spectrometer to record the signal levels. The absolute photon flux was measured using an XUV photodiode (IRD AXUV100). Figure 4 shows the continua spectra using the DOG and PG method. A spectrum of the attosecond pulse train produced by the linearly polarized field is also plotted for comparison, but the harmonic peaks are not seen in the spectrum region above 100 eV

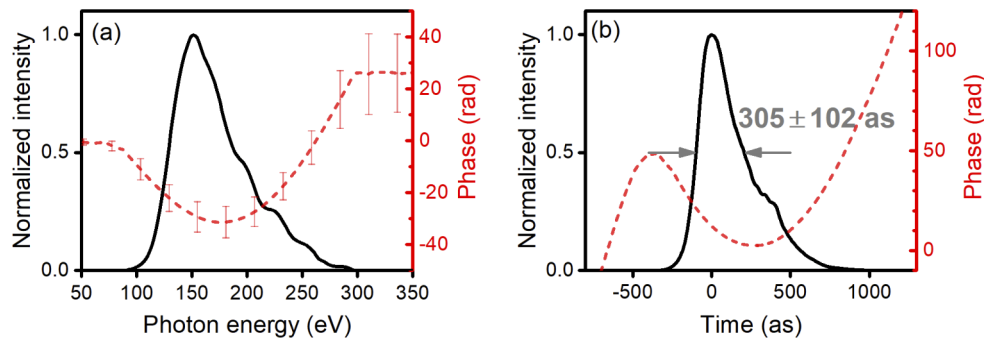


Fig. 3. Attosecond pulse retrieval with neural network using the measured streaking trace in Fig. 2(b). (a) Neural network retrieved photon spectrum and spectrum phase; photoionization potential and cross section of helium are considered to correct the photon spectra. (b) Temporal intensity profile and temporal phase of the 305 as pulse.

due to the limited resolution of the spectrometer and the low photon energy of the mid-IR laser. All three spectra were detected under same detection conditions. In all three cases, the CEP value, gas cell position and iris size were optimized individually to achieve the best maximum flux near 150 eV, which corresponds to the peak in the HHG plateau.

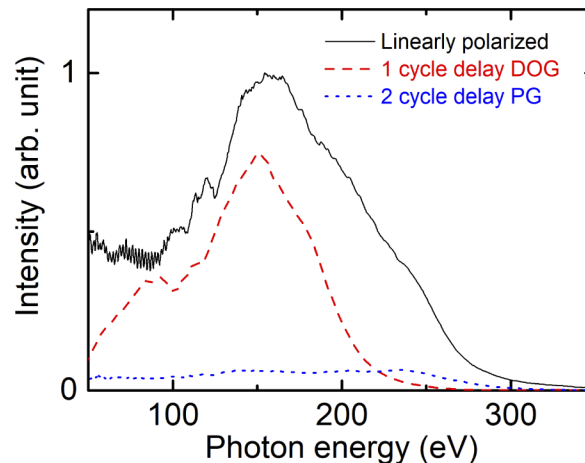


Fig. 4. The photon spectrum of an attosecond pulse train generated using a linearly polarized field (solid black); The photon spectrum of IAPs generated using a DOG field with one-cycle delay (solid red) and a PG field with two-cycle delay (dashed blue). In each case, the CEP value, gas cell position and iris size were optimized individually to achieve the best maximum flux near 150 eV.

In interferometric DOG, the attosecond spectra shape and cutoff energy can be optimized by fine tuning the relative phase between the SH and the driving field [32]. In our collinear DOG case, this relative phase is fixed to ensure shot-to-shot stability of the HHG. We believe the inability to fine tuning the relative phase between the driving field and the SH field is the main reason for lower cutoff energy in our collinear DOG, which can be solved by testing different combinations of the BBO crystal and the second quartz with varying thickness.

In our typical experimental condition, the pulse energy of the linear polarized driving field is approximately 0.8 mJ measured after the lens. In the PG case, the pulse energy required to reach 300 eV is usually near 1.1 mJ. In the DOG case, the 100-250 eV photons are typically optimized

with 0.9 mJ of driving field, resulting a 0.3 nJ soft X-ray attosecond pulse with a photon flux of $\sim 1.5 \times 10^7$ photons per laser shot. The conversion efficiency for the IAPs reaches 2×10^{-7} in the DOG case, which is more than one order of magnitude higher than the two-cycle delay PG case demonstrated previously [20]. We compared the driving and gating fields in one and two-cycle delay cases. For the same driving field intensity inside the gate, the electric field strength in the leading edge is smaller in the DOG case (Fig. 5). Therefore, the ground state depletion can be reduced accordingly. This is the main reason for a higher IAP flux in DOG with one-cycle delay.

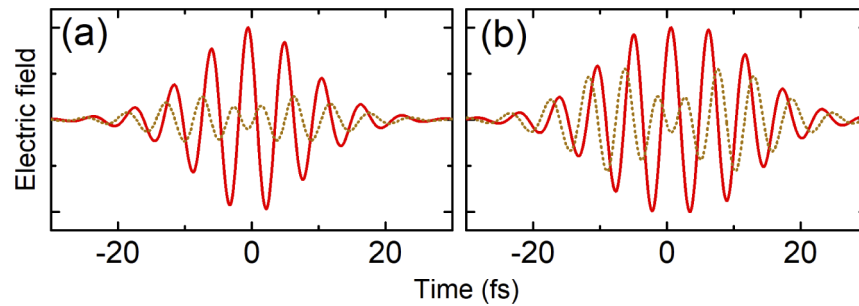


Fig. 5. The driving (red solid) and gating field (yellow dotted) in (a) one-cycle delay case and (b) two-cycle delay case.

4. Conclusion

In this work, the DOG technique was implemented for the first time with a mid-IR laser source at 1.7 μm . Although the DOG technique was invented initially for generating IAPs with multicycle laser sources. We have demonstrated its potential to generate high flux soft X-ray IAPs with a two-cycle mid-IR laser. The photon energy of the IAP in 100–250 eV range reaches 0.3 nJ, corresponding to a photon flux of $\sim 1.5 \times 10^7$ photons per laser shot and a conversion efficiency of 2×10^{-7} with 1.5 mJ of available mid-IR energy. The DOG method discussed in this letter is also practical with higher pulse energy. We believe it can be adapted to the next generation of attosecond sources in large scale laser facilities [33].

Funding

Air Force Office of Scientific Research (FA9550-15-1-0037, FA9550-16-1-0013); Army Research Office (W911NF-14-1-0383, W911NF-19-1-0224); Defense Advanced Research Projects Agency (D18AC00011); National Science Foundation (1806575); CAS Pioneer Hundred Talents Program (2018-131-S).

Disclosures

The authors declared that they have no conflicts of interest to this work.

References

1. P. M. Paul, E. Toma, P. Breger, G. Mullot, F. Augé, P. Balcou, H. Muller, and P. Agostini, "Observation of a train of attosecond pulses from high harmonic generation," *Science* **292**(5522), 1689–1692 (2001).
2. M. Hentschel, R. Kienberger, C. Spielmann, G. Reider, N. Milosevic, T. Brabec, P. Corkum, U. Heinzmann, M. Drescher, and F. Krausz, "Attosecond metrology," *Nature* **414**(6863), 509–513 (2001).
3. Z. Chang, P. B. Corkum, and S. R. Leone, "Attosecond optics and technology: progress to date and future prospects [Invited]," *J. Opt. Soc. Am. B* **33**(6), 1081–1097 (2016).
4. C. Francesca, S. Giuseppe, S. Salvatore, V. Caterina, and N. Mauro, "Advances in attosecond science," *J. Phys. B: At., Mol. Opt. Phys.* **49**(6), 062001 (2016).

5. E. Goulielmakis, M. Schultze, M. Hofstetter, V. S. Yakovlev, J. Gagnon, M. Uiberacker, A. L. Aquila, E. Gullikson, D. T. Attwood, and R. Kienberger, "Single-cycle nonlinear optics," *Science* **320**(5883), 1614–1617 (2008).
6. A. Jullien, T. Pfeifer, M. J. Abel, P. Nagel, M. Bell, D. M. Neumark, and S. R. Leone, "Ionization phase-match gating for wavelength-tunable isolated attosecond pulse generation," *Appl. Phys. B: Lasers Opt.* **93**(2-3), 433–442 (2008).
7. P. Corkum, N. Burnett, and M. Y. Ivanov, "Subfemtosecond pulses," *Opt. Lett.* **19**(22), 1870–1872 (1994).
8. H. Mashiko, S. Gilbertson, C. Li, S. D. Khan, M. M. Shakya, E. Moon, and Z. Chang, "Double optical gating of high-order harmonic generation with carrier-envelope phase stabilized lasers," *Phys. Rev. Lett.* **100**(10), 103906 (2008).
9. P. B. Corkum, "Plasma perspective on strong field multiphoton ionization," *Phys. Rev. Lett.* **71**(13), 1994–1997 (1993).
10. K. S. Budil, P. Salières, A. L'Huillier, T. Ditmire, and M. D. Perry, "Influence of ellipticity on harmonic generation," *Phys. Rev. A* **48**(5), R3437–R3440 (1993).
11. P. Balcou, P. Salieres, A. L'Huillier, and M. Lewenstein, "Generalized phase-matching conditions for high harmonics: The role of field-gradient forces," *Phys. Rev. A* **55**(4), 3204–3210 (1997).
12. S. L. Cousin, N. Di Palo, B. Buades, S. M. Teichmann, M. Reduzzi, M. Devetta, A. Kheifets, G. Sansone, and J. Biegert, "Attosecond Streaking in the Water Window: A New Regime of Attosecond Pulse Characterization," *Phys. Rev. X* **7**(4), 041030 (2017).
13. K. T. Kim, C. Zhang, T. Ruchon, J.-F. Hergott, T. Auguste, D. Villeneuve, P. Corkum, and F. Quéré, "Photonic streaking of attosecond pulse trains," *Nat. Photonics* **7**(8), 651–656 (2013).
14. H. Vincenti and F. Quéré, "Attosecond Lighthouses: How To Use Spatiotemporally Coupled Light Fields To Generate Isolated Attosecond Pulses," *Phys. Rev. Lett.* **108**(11), 113904 (2012).
15. M. Schultze, M. Fieß, N. Karpowicz, J. Gagnon, M. Korbman, M. Hofstetter, S. Neppl, A. L. Cavalieri, Y. Komninos, T. Mercouris, C. A. Nicolaides, R. Pazourek, S. Nagele, J. Feist, J. Burgdörfer, A. M. Azzeer, R. Ernstorfer, R. Kienberger, U. Kleineberg, E. Goulielmakis, F. Krausz, and V. S. Yakovlev, "Delay in Photoemission," *Science* **328**(5986), 1658–1662 (2010).
16. B. Shan and Z. Chang, "Dramatic extension of the high-order harmonic cutoff by using a long-wavelength driving field," *Phys. Rev. A* **65**(1), 011804 (2001).
17. Y. Pertot, C. Schmidt, M. Matthews, A. Chauvet, M. Huppert, V. Svoboda, A. von Conta, A. Tehlar, D. Baykusheva, J.-P. Wolf, and H. J. Wörner, "Time-resolved x-ray absorption spectroscopy with a water window high-harmonic source," *Science* **355**(6322), 264–267 (2017).
18. A. Chew, N. Douguet, C. Cariker, J. Li, E. Lindroth, X. Ren, Y. Yin, L. Argenti, W. T. Hill, and Z. Chang, "Attosecond transient absorption spectrum of argon at the $L_{2,3}$ edge," *Phys. Rev. A* **97**(3), 031407 (2018).
19. F. Silva, S. M. Teichmann, S. L. Cousin, M. Hemmer, and J. Biegert, "Spatiotemporal isolation of attosecond soft X-ray pulses in the water window," *Nat. Commun.* **6**(1), 6611 (2015).
20. J. Li, X. Ren, Y. Yin, K. Zhao, A. Chew, Y. Cheng, E. Cunningham, Y. Wang, S. Hu, Y. Wu, M. Chini, and Z. Chang, "53-attosecond X-ray pulses reach the carbon K-edge," *Nat. Commun.* **8**(1), 186 (2017).
21. T. Gaumnitz, A. Jain, Y. Pertot, M. Huppert, I. Jordan, F. Ardana-Lamas, and H. J. Wörner, "Streaking of 43-attosecond soft-X-ray pulses generated by a passively CEP-stable mid-infrared driver," *Opt. Express* **25**(22), 27506–27518 (2017).
22. A. S. Johnson, D. R. Austin, D. A. Wood, C. Brahm, A. Gregory, K. B. Holzner, S. Jarosch, E. W. Larsen, S. Parker, and C. S. Strüber, "High-flux soft x-ray harmonic generation from ionization-shaped few-cycle laser pulses," *Sci. Adv.* **4**(5), eaar3761 (2018).
23. A. D. Shiner, C. Trallero-Herrero, N. Kajumba, H. C. Bandulet, D. Comtois, F. Légaré, M. Giguère, J. C. Kieffer, P. B. Corkum, and D. M. Villeneuve, "Wavelength Scaling of High Harmonic Generation Efficiency," *Phys. Rev. Lett.* **103**(7), 073902 (2009).
24. M. Möller, Y. Cheng, S. D. Khan, B. Zhao, K. Zhao, M. Chini, G. G. Paulus, and Z. Chang, "Dependence of high-order-harmonic-generation yield on driving-laser ellipticity," *Phys. Rev. A* **86**(1), 011401 (2012).
25. J. Mauritsson, P. Johnsson, E. Gustafsson, A. L'Huillier, K. J. Schafer, and M. B. Gaarde, "Attosecond Pulse Trains Generated Using Two Color Laser Fields," *Phys. Rev. Lett.* **97**(1), 013001 (2006).
26. Y. Yin, J. Li, X. Ren, K. Zhao, Y. Wu, E. Cunningham, and Z. Chang, "High-efficiency optical parametric chirped-pulse amplifier in BiB 3 O 6 for generation of 3 mJ, two-cycle, carrier-envelope-phase-stable pulses at 1.7 μm ," *Opt. Lett.* **41**(6), 1142–1145 (2016).
27. Z. Chang, "Single attosecond pulse and xuv supercontinuum in the high-order harmonic plateau," *Phys. Rev. A* **70**(4), 043802 (2004).
28. J. Li, X. Ren, Y. Yin, Y. Cheng, E. Cunningham, Y. Wu, and Z. Chang, "Polarization gating of high harmonic generation in the water window," *Appl. Phys. Lett.* **108**(23), 231102 (2016).
29. C. A. Haworth, L. E. Chipperfield, J. S. Robinson, P. L. Knight, J. P. Marangos, and J. W. G. Tisch, "Half-cycle cutoffs in harmonic spectra and robust carrier-envelope phase retrieval," *Nat. Phys.* **3**(1), 52–57 (2007).
30. J. White and Z. Chang, "Attosecond streaking phase retrieval with neural network," *Opt. Express* **27**(4), 4799–4807 (2019).
31. Y. Mairesse, A. De Bohan, L. Frasiniski, H. Merdji, L. Dinu, P. Monchicourt, P. Breger, M. Kovačev, R. Taïeb, and B. Carré, "Attosecond synchronization of high-harmonic soft x-rays," *Science* **302**(5650), 1540–1543 (2003).
32. S. Gilbertson, H. Mashiko, C. Li, S. D. Khan, M. M. Shakya, E. Moon, and Z. Chang, "A low-loss, robust setup for double optical gating of high harmonic generation," *Appl. Phys. Lett.* **92**(7), 071109 (2008).
33. K. Sergej, D. Mathieu, K. Subhendu, M. Sudipta, F. Miklós, C. Tamás, F. Balázs, M. Balázs, V. Zoltán, C. Eric, K. Mikhail, C. Francesca, D. Michele, F. Fabio, M. Erik, P. Luca, S. Salvatore, V. Caterina, N. Mauro, R. Piotr, M. Sylvain, C. Filippo, W. Hampus, L. A. Cord, M. H. Christoph, J. Per, L. H. Anne, L.-M. Rodrigo, H. Stefan,

B. Maïmona, B. Frederik, V. Aline, I. Gregory, S. Emmanuel, P. Nikos, K. Constantinos, T. Paraskevas, L. Franck, C. Dimitris, V. Katalin, O. Károly, and S. Giuseppe, "The ELI-ALPS facility: the next generation of attosecond sources," *J. Phys. B: At., Mol. Opt. Phys.* **50**(13), 132002 (2017).